

Improvement of Mechanical Properties of Linear Low-Density Polyethylene (LLDPE) Films by Addition of Montmorillonite-Erucamide Nanocomposite (MMT-EU)

Leticia Bavaresco Cima^a, Pahola Patussi^b, Glaucea Warmeling Duarte^c ,
Éverton Rafael Breitenbach^a, Abel Andre Candido Recco^d , Luciano Luiz Silva^e ,
Micheli Zanetti^e , Gustavo Lopes Colpani^{b,e} , Josiane Maria Muneron de Mello^{b,e} ,
Thiago André Carniel^a , Márcio Antônio Fiori^{b,e,f,*} 

^aUniversidade Comunitária da Região de Chapecó (Unochapecó), Escola Politécnica, Chapecó, SC, Brasil.

^bUniversidade Comunitária da Região de Chapecó (Unochapecó), Programa de Pós-Graduação em Ciências Ambientais, Chapecó, SC, Brasil.

^cCentro Universitário Barriga Verde (UNIBAVE), Centro de Pesquisa em Engenharia, Orleans, SC, Brasil.

^dUniversidade do Estado de Santa Catarina (UDESC), Centro de Ciências Tecnológicas, Joinville, SC, Brasil.

^eUniversidade Comunitária da Região de Chapecó (Unochapecó), Programa de Pós-Graduação em Tecnologia e Gestão da Inovação, Chapecó, SC, Brasil.

^fUniversidade Tecnológica Federal do Paraná (UTFPR), Departamento de Física, Pato Branco, PR, Brasil.

Received: December 15, 2022; Revised: April 13, 2023; Accepted: July 18, 2023

The Montmorillonite-Erucamide nanocomposite (MMT-EU) can be used to reduce and to control the values of coefficient of friction of low-density polyethylene films (LDPE), widely used by the food industry. In this work, the effect of the addition of 5 wt% and 10 wt% of MMT-EU on the mechanical properties of LLDPE films involving the weld region was investigated. The MMT-EU concentration range was defined considering its possible technological application as an additive to stabilize the friction coefficient of polymeric films. The result shows a significant improvement in the values of stiffness, strength and ductility of polymeric films. In addition, it did not change the coefficient of friction, but the brightness of the LLDPE films decreased and the opacity increased, due to the increase in the crystallinity degree of the LLDPE polymer promoted by MMT-EU, not being a problem for the application of these films.

Keywords: linear low-density polyethylene (LLDPE), erucamide, nanocomposite, mechanical properties.

1. Introduction

Polymeric films produced with Low-Density Polyethylene (LDPE) are widely used in the manufacture of various products, especially in the packaging used by the food industry. The production of these films requires particular polymeric materials and special processes to obtain products with good physical and chemical properties, at a low cost. In particular, important surface properties are required for LDPE films when applied to packaging, for example, roughness and coefficient of friction (COF), associated with good mechanical resistance¹.

In order to improve the surface and mechanical properties of polymeric films additives are incorporated into material formulations. To adjust the coefficient of friction of polyethylene films fatty acid amides are commonly used due to their strong tendency to migrate to the surface, such as erucamide molecules. Erucamide molecules influence the performance of polymeric surfaces, being classified as a powerful slip additive, as it forms smooth placoid-type crystals on the polymeric surface, which causes reduction

in the coefficient of friction^{2,3}. However, the coefficient of friction does not necessarily depend on the surface coating of the film by the erucamide, as different erucamide crystals can be formed, similar to plaques, which also modify the COF values⁴.

However, the erucamide molecules are not compatible with polyethylene and polypropylene polymers due to their chemical structure, which have polar functional groups. This characteristic difficult its distribution and homogenization on the polymer matrix and causes the formation of large agglomerates on the polymeric surface. Thus, its addition to polyethylene films improves the coefficient of friction but impairs the mechanical properties⁵.

However, erucamide molecules are highly mobile in nonpolar polymers and, therefore, the values of the coefficient of friction on the surfaces of these polymers change quickly, which can have negative consequences for packaging manufacturing processes, for example. It has been demonstrated that the concentration of erucamide on the surface of linear low-density polyethylene films (LLDPE films) has a direct relationship with the values of the coefficient of friction,

*e-mail: marciofiori@utfpr.edu.br

with a critical surface concentration of erucamide being $0.5 \text{ g}\cdot\text{cm}^{-2}$, being that with higher values having a negligible effect on the coefficient of friction⁶.

To mitigate these disadvantages, it is possible to employ surface modifiers. These modifiers, in order to reduce the erucamide migration rate to the polyethylene surface, must have a nonpolar chain, in addition to a high molecular weight, in order to be efficient in compatibilizing and retaining erucamide in the polyethylene matrix, for example. Thus, the intercalation of erucamide molecules with the nanoclay is a good strategy to obtain a nanocomposite called MMT-EU, which is compatible with nonpolar polyethylene matrices and with erucamide phases, and which is therefore a good compatibilizer.

Recently, Silvano et al.⁷ reported that the MMT-EU nanocomposite is compatible with the erucamide phases and compatible with the polyethylene polymer and improves some surface properties, as the coefficient of friction and the optical properties of the linear low-density polyethylene films^{7,8}.

It is known that the incorporation of montmorillonite in polymeric matrices improves the dispersion of nonpolar additives and to increase the mechanical properties of the polymer. In turn, montmorillonite reduces the presence of agglomerates and even air bubbles, which result in incompatibility between the polymers and the additives and impair the mechanical properties⁹. But very high clay concentrations can reduce the tensile strength and strain at break of the polymeric matrix. Therefore, it is necessary to consider the relationship between the amount of montmorillonite and the polymer, with a view on the desired mechanical properties¹⁰.

Recent studies have shown that with the combination of montmorillonite and erucamide it is possible to obtain a nanocomposite called MMT-EU, which can be a good and promising additive to improve the surface characteristics of LLDPE films, used in the manufacture of flexible packaging, and at the same time improving the mechanical properties of polymers^{7,11}.

Therefore, this work was dedicated to evaluating the effect of the montmorillonite-erucamide nanocomposite (MMT-EU) on the mechanical properties of the LLDPE films made with one welding region, considering that recent works showed that the addition of the MMT-EU nanocomposite improves the miscibility of the erucamide molecules in the LLDPE matrix and improves its surface properties. Thus, in this work, the incorporation of different percentages of the MMT-EU in the LLDPE films was evaluated, and simultaneously, the characterization of the MMT-EU nanocomposite and of the LLDPE films was made.

2. Materials and Methods

2.1. Montmorillonite-erucamide nanocomposite (MMT-EU)

The montmorillonite-erucamide nanocomposite (MMT-EU) was produced with 15 wt% of a commercial Cloisite 20A montmorillonite (Bun Tech – particle size minor that $2 \mu\text{m}$, x-ray diffraction d-spacing (001) of 31.5 \AA , from $2\theta = 3.65^\circ$, Bulk Density of 0.118 g/cc) and with 85 wt% of powder erucamide (CRODA), by the process of intercalation

of the erucamide molecules in the montmorillonite structures, according to the methodology proposed by Silvano et al.⁷. The intercalation processes were carried out in a glass reactor at 100°C , with mechanical agitation at 3000 rpm for 60 minutes and with temperature controlled by a glycerin water bath. In Figure 1a an image of the MMT-EU nanocomposite is shown.

Once the MMT-EU nanocomposite was synthesized and after a masterbatch was prepared with the MMT-EU and with Low-Density Polyethylene (LDPE, Braskem) using a single-screw extrusion system with $L/D = 22$, with four zones heating: 135, 144, 146 and 154°C and with a rotation speed of 45 rpm. In this procedure, 85 wt% of LDPE was blended with 15 wt% of MMT-EU nanocomposite and resulting in a masterbatch LDPE/MMT-EU granules, Figure 1b.

In order, to characterize the MMT-EU nanocomposite the samples were submitted to analysis by x-ray diffraction (XRD), Fourier transform infrared spectroscopy (FT-IR) and transmission electron microscopy (TEM).

Presence of intercalated and/or exfoliated structures in the MMT-EU nanocomposite were evaluated using the XRD technique. The XRD analysis was performed using an x-ray powder diffraction diffractometer (D8, Bruker, USA) with $\text{CuK}\alpha$ radiation at tension of 40 kV and electrical current of 40 mA, with 1.54 \AA wavelength and with a step of 0.02° in the 2θ range from 2 to 15° at room temperature.

The functional groups of the erucamide molecules, montmorillonite, MMT-EU nanocomposite were analyzed by Fourier transform infrared (FT-IR 4200, Jasco, Japan) spectrophotometer between 4000 cm^{-1} and 400 cm^{-1} . All samples were prepared in potassium bromide (KBr) and submitted following conventional protocols.

Details of the montmorillonite nanoparticles with the erucamide molecules intercalated were observed with TEM images. The TEM images were obtained with a TEM microcopy (JEM-2100 TEM 200 kV - JEOL). The samples were dispersed in a beaker with distilled water and sonicated for 30 s. Using a pipette, a drop of this solution was deposited on a 200 # grid and then dried for 24 h.

2.2. Linear low-density polyethylene films (LLDPE films)

2.2.1. Preparation of the films

The polymeric films were obtained with the Linear Low-Density Polyethylene (LLDPE, Braskem) with the LDPE/



Figure 1. (a) montmorillonite-erucamide nanocomposite (MMT-EU) produced with 15 wt% of montmorillonite (Cloisite 20A) and with 85 wt% of erucamide – magnification of 20 times. (b) masterbatch (LDPE/MMT-EU) produced with 85 wt% of LDPE and with 15 wt% of MMT-EU nanocomposite - magnification of 10 times.

MMT-EU masterbatch with different mass percentages: 0 wt%, 5 wt% and 10 wt%. These blends were defined as LLDPE films (0 wt%), LLDPE with 5 wt% of LDPE/MMT-EU and LLDPE with 10 wt% of LDPE/MMT-EU, respectively.

The films were manufactured in a balloon-type single-screw extruder (Oryzon) with a rotation speed of 93 rpm and with a temperature profile: 185, 185, 185, 185, 185, 190 and 205 °C, respectively. The material was extruded vertically through a ring-shaped die, in which a constant jet of air was used to balloon-expand the melt. After stretching and cooling, the resulting tubular film was wound onto bobbins.

Aiming at technological applications in the food industry, for example, flexible polymeric packages were made for all compositions. In this process, the films were welded and the packages were obtained with the same dimension and characteristics, Figure 2. The welding was performed on a sealer (Microvac Selovac) with a Teflon® weld region at 180°C and with a residence time of 1.6 seconds.

2.2.2. Characterization of the films

Differential scanning calorimetry (DSC) was used to evaluate the effect of the percentage of MMT-EU on the melting temperature and on the crystallization temperature and on the enthalpy of fusion and on the enthalpy of crystallization of the LLDPE films. The thermal analyses were carried out by means of a differential scanning calorimeter (DSC-Perkin Elmer, USA) under a nitrogen atmosphere. The heating-cooling-reheating methodology was employed in the DSC experiments to eliminate the thermal history of the samples. The sample were heated with two temperature cycle from 30 °C to 180 °C at a heating rate of 10 °C.min⁻¹ and with one cooling step with cooling rate of 5 °C.min⁻¹. The DSC thermograms from the second heating of the samples were then analyzed to obtain the melting temperature (T_m),

crystallization temperature (T_c), enthalpy of fusion (ΔH_m) and enthalpy of crystallization (ΔH_c) of the samples.

Analyses with atomic force were performed on the LDPE films, LDPE films with 5 wt% of LDPE/MMT-EU and with 10 wt% of LDPE/MMT-EU. The average roughness value for the surface of the LLDPE with different percentages of LDPE/MMT-EU were determined. The information on the topography and roughness of the films was obtained using an atomic force microscope (NanoSurf, model Nanite B). The film surface scanning configuration was in contact mode with a load of 11.16nN. The topography images were acquired by the NanoSurf CETR AFM software with dimensions of 3µm x 3µm and pixel size of approximately 6nm. The average roughness was obtained with the aid of the Nanosurf C3000 software.

Contact angle measurements were performed for the surfaces of LLDPE films, LLDPE with 5 wt% of LDPE/MMT-EU and LLDPE with 10 wt% of LDPE/MMT-EU. The average contact angle values were determined for the water drops on the LDPE films surfaces with and without MMT-EU. Contact angles were determined using a Ramé-Hart goniometer (model 590 of the F4 series) with images being obtained from drops of deionized water (0.83 µL) on the surface of each sample. For each test, a series of photos was obtained with time intervals of 1 second, and for each drop on the surface 30 measurements were taken in a total interval of 30 seconds.

For the tensile tests 12 samples were obtained from the polymeric packages and for the compositions LLDPE films (0 wt%), LLDPE with 5 wt% and LDPE/MMT-EU with 10 wt%. Each sample consists of 300 x 35 mm strip cut off from the polymeric packages, in which the welded region is located in the middle plane of the sample, Figure 3.

Tensile tests were performed at room temperature (~25 °C) in a universal testing machine (AGX Plus, Shimadzu). In order to avoid sliding of the samples during the tests, common adhesive tape was applied at the clamping site. Each sample was fixed with a clamp-to-clamp distance of 200 mm, keeping the welded region in the middle plane. Thereafter, a pre-loading of 1.0 N was imposed in order to hold the film straight, and the tensile experiments was performed, consisting of a displacement controlled monotonic test. In detriment of classical low-rate tests, a displacement rate of 1000 mm.min⁻¹ was imposed in order to induce higher mechanical loadings at the welding region.

The surface deformation of each sample was recorded by a CMOS sensor camera (monochromatic, 2 MP, 30 FPS). The kinematic measurements were performed in the DIC software *GOM Correlate* (ZEISS Group), where the



Figure 2. Polymeric packages made with the films thermally welded. Example: for the composition LLDPE with 10 wt% of LDPE/MMT-EU.

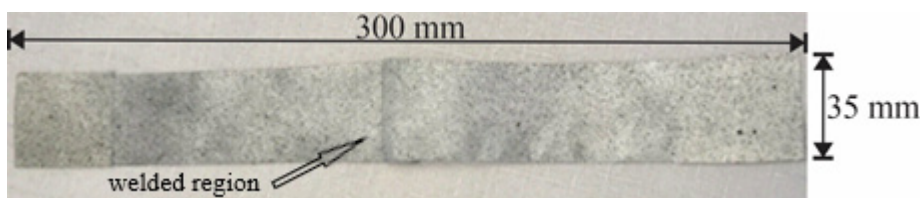


Figure 3. Sample with 300 x 35 mm strip cut off from the polymeric packages, in which the welded region is located in the middle plane of the sample. Example: for the composition LLDPE with 10 wt% of LDPE/MMT-EU.

stochastic speckle pattern was obtained by spraying a black paint on the surface of the specimens, Figure 3.

Mechanical responses investigated were threefold: i) the non-linear stiffness up to the softening threshold, ii) the strain distributions close to the welding and iii) the force and displacement at the softening point (prior cold-drawing). The proposed approach for each one of them is described in the sequence.

Since the mechanical response is clearly non-linear and finite strains take place the use of the classical *Young's modulus* - retrieved from the linear elasticity theory¹² to characterize the stiffness at the constitutive level, is highly questionable in such a case. In this regard, the following exponential relation is proposed to represent the force-displacement response resulting from the tests:

$$F(u) = \frac{k}{\alpha} (1 - e^{-\alpha u}), \quad \frac{dF}{du} = ke^{-\alpha u}, \quad (1)$$

where F is the force, u is the displacement and $\{k, \alpha\}$ is the set of fitting parameters. The Equation 1 was employed to fit each of the tested samples up to the softening threshold, i.e., $u \approx 30$ mm. The parameters identification was based on a nonlinear curve fitting procedure, where the exponent $\alpha = 0.0954$ was fixed for all curves. Therefore, only the parameter k can be used to measure the stiffness of each curve.

Concerning the strain fields retrieved from the DIC analyses, a region of interest (ROI) was defined close to the welded region. In these analyses, the von Mises measure of the Hencky (logarithmic) strain $\varepsilon = \ln(V)$ was used, where $V = FF^T$ is the left Cauchy-Green stretch tensor and F is the deformation gradient^{9,10}. One representative of each set of samples tested was analyzed regarding their distribution, looking at the overall values within the ROI up to 25% of clamp elongation.

The forces and displacements at the softening point were directly acquired from the force-displacement curves. Earlier analyses of mechanical data, based on both Lilliefors test and quantile-quantile diagrams (Q-Q plot), point out non-normal distributions. Accordingly, the statistical significances ($p < 0.05$) among compositions were verified using the classical nonparametric Wilcoxon's test.

In addition to the previous mentioned characterization, the samples from the polymeric packages were also analyzed regarding friction, brightness and opacity. The coefficients of friction were assessed according to ASTM D1894. Brightness and opacity were measured according to ASTM D2457.

3. Results and Discussions

3.1. Characterization of the MMT-EU nanocomposite

3.1.1. Transmission Electron Microscopy (TEM)

Figure 4 shows the TEM images obtained with the MMT-EU nanocomposite. The images show small clusters of montmorillonite nanoparticles with dimensions between 200 nm and 500 nm are dispersed in the erucamide phase, Figure 4a. Figure 4b shows details and reveals that the clusters are formed by rod-shaped MMT nanoparticles with a diameter

between 20-30 nm and lengths between 100-200 nm. At the interface between the rod-shaped MMT nanoparticles and the erucamide phase no significant defects are observed, which is a strong indication of a good compatibility of the MMT nanocomposite with the erucamide phase, Figure 4c.

3.1.2. X-ray diffraction (XRD)

The x-ray diffractograms obtained with the montmorillonite nanoparticles, with the erucamide and with MMT-EU nanocomposite are shown in Figure 5. The x-ray diffractogram for the montmorillonite nanoparticles shows a characteristic diffraction peak at 2θ equal to 7.12° , which is associated with the diffraction by the interplanar layers¹³. The characteristic diffraction peaks for erucamide are observed at 2θ equal to 6.00° and 11.00° ¹⁴.

It is evident that the mixture between montmorillonite and erucamide does not cause significant changes in the characteristic diffraction peaks. These results suggest the formation of the MMT-EU nanocomposite, which is in agreement with the work reported by Silvano et al.⁷. From the XRD analysis, it is also possible to conclude that after the mixing process, the montmorillonite nanoparticles and the erucamide molecules maintain their chemical and physical integrity, since the peaks obtained for the nanocomposite are well defined and maintain the character of a pure compound.

3.1.3. Fourier transform infrared spectroscopy (FT-IR)

In Figure 6 are shown the FT-IR spectra obtained with the montmorillonite nanoparticles, with erucamide and with MMT-EU nanocomposite. Typical and principal transmittance bands for the erucamide molecules are observed at 3390 cm^{-1} and at 3305 cm^{-1} , associated with the vibrations of the NH_2 groups. In 1638 cm^{-1} there is a strong and narrow band, that represents the axial deformation of N-C=O bonds, both presents in the amide functional group. In 1452 cm^{-1} are observed a strong band associated with the aliphatic C-H of the methylene group and at 1400 cm^{-1} a band associated with the aliphatic C-H of the methyl group¹³.

FT-IR obtained with the montmorillonite nanoparticles is characteristic of a clay mineral. At the wavelength of 3632 cm^{-1} there is a weak and wide transmission band that is associated with the vibrational modes of the hydroxyl groups adsorbed on the structure.

In the wavelengths of 2927 cm^{-1} and 2855 cm^{-1} there are a medium and narrow band associated with the vibrations of the methyl (CH_3) and methylene (CH_2) groups, respectively. The wide and weak bands present in the wavelength of 2246 cm^{-1} are related to the vibrational modes of the $\text{C}\equiv\text{N}$ groups and the narrow and strong band present in 1040 cm^{-1} corresponds to the vibrational modes of the Si-O groups¹⁵.

3.2. Characterization of the LLDPE films with MMT-EU nanocomposite

3.2.1 Fourier transform infrared spectroscopy (FT-IR)

The FT-IR spectra obtained for the LLDPE films and for the LLDPE films with 5 wt% and 10 wt% of LDPE/MME-EU are shown in Figure 7. The presence of transmittance bands at 3390 cm^{-1} and at 3305 cm^{-1} are associated with the vibration modes of the NH_2 groups, and at 1638 cm^{-1} is associated with

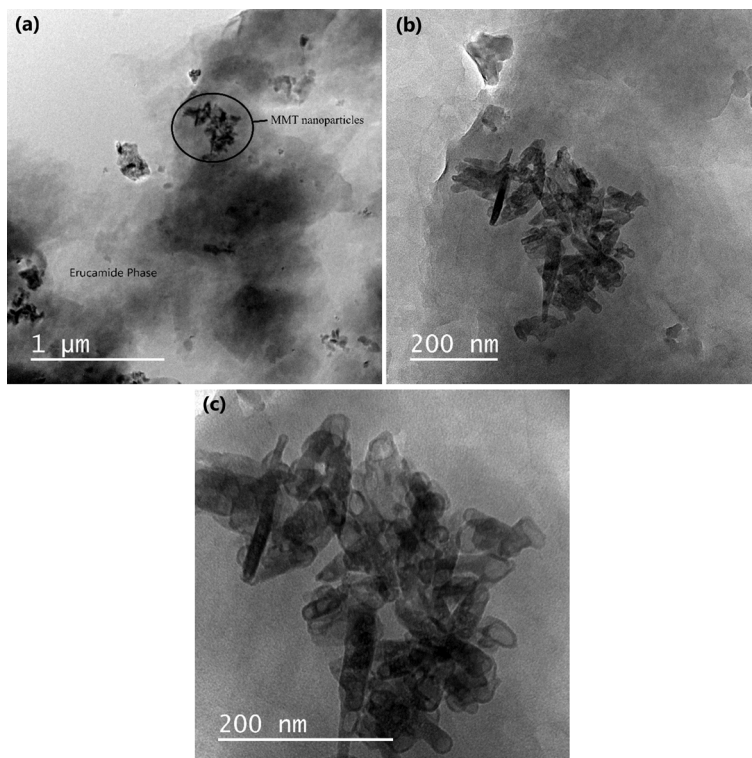


Figure 4. Transmission electronic images obtained with the montmorillonite-erucamide nanocomposite (MMT-EU). (a) MMT nanoparticles dispersed in the erucamide phase, (b) details of a cluster of MMT nanoparticles, and (c) details of rod-shaped MMT nanoparticles with a diameter between 20-30 nm and a length between 100 nm and 200 nm.

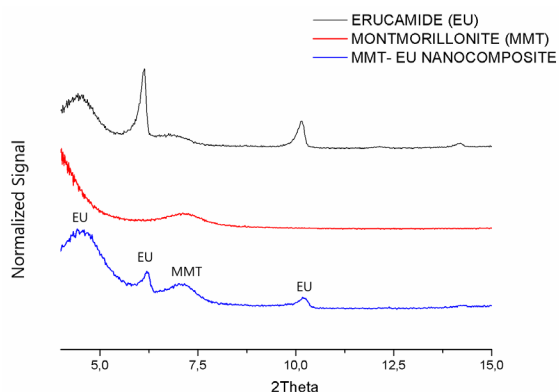


Figure 5. X-ray diffractograms with normalized signal, obtained for montmorillonite nanoparticles, for erucamide and for the MMT-EU nanocomposite.

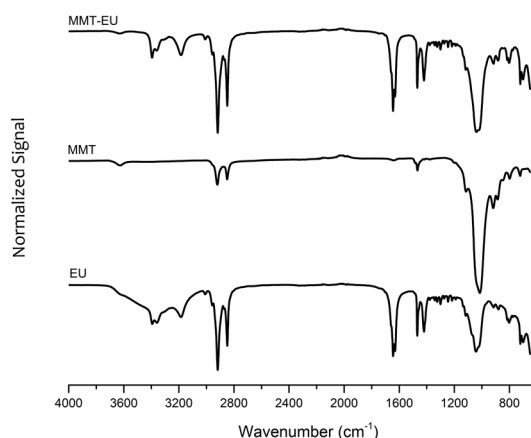


Figure 6. FT-IR spectrums with normalized signal, obtained for the montmorillonite nanoparticles, for the erucamide and for the MMT-EU nanocomposite.

the axial deformations of the N-C=O bonds, all chemical groups present in the erucamide molecules of the MMT-EU nanocomposite. The increase in the concentration of MMT-EU in the LLDPE films promotes the increase of the magnitude of these transmittance bands, confirming the presence of the MMT-EU nanocomposite in the polymeric films.

The FTIR spectra confirm the chemical integrity of LLDPE and MMT-EU and prove that there are only physical interactions between the polymeric molecules and the molecules of the nanocomposite.

3.2.2. Differential scanning calorimetry (DSC)

The DSC thermograms in Figure 8 show the thermal behavior of LLDPE and LLDPE films with different concentrations of LDPE/MMT-EU. The melting temperature and crystallization temperature of LLDPE films are practically the same as LLDPE films with 5 wt% and 10 wt% of LDPE/MMT-EU. The values of enthalpy of fusion and enthalpy of crystallization show important variations that provide improvement in the mechanical properties of LLDPE films. The corresponding thermal property values are shown in Table 1.

With the addition of 5 wt% of LDPE/MMT-EU, the enthalpy of fusion and the enthalpy of crystallization of the LLDPE films decrease by 14.06% and 18.79%, respectively. But with a higher percentage of LDPE/MMT-EU (10 wt%),

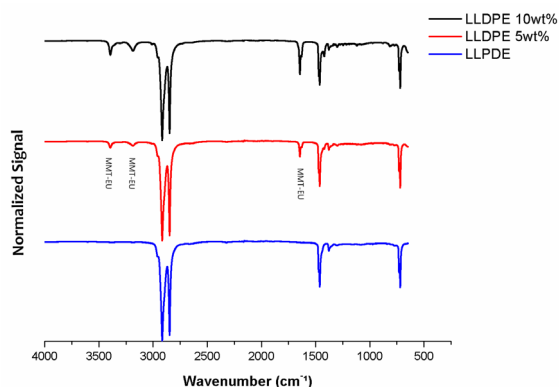


Figure 7. FT-IR spectrums with normalized signal, obtained for the LLDPE films and for the LLDPE films with 5 wt% and 10 wt% of LDPE/MME-EU nanocomposite.

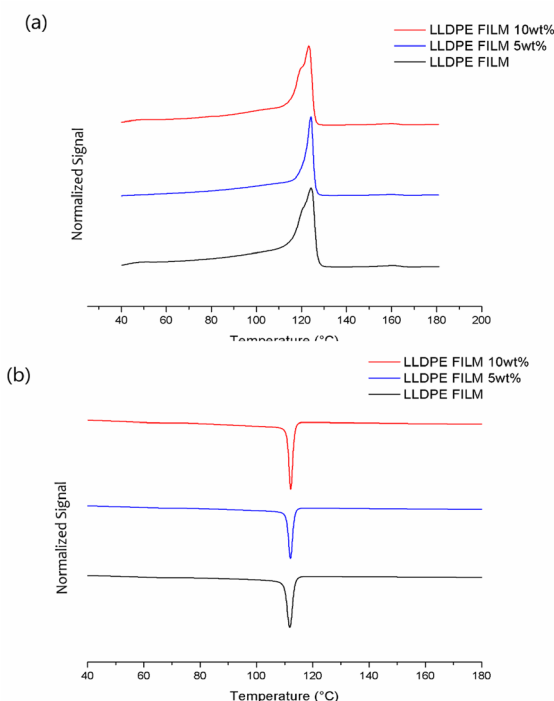


Figure 8. Thermal behavior of the LLDPE films and of the LLDPE with different concentrations of LDPE/MMT-EU. (a) DSC thermogram with normalized signal for the second heating and (b) DSC thermogram with normalized signal for the first cooling.

Table 1. Thermal properties determined by DSC analysis of the LLDPE films and of the LLDPE films with 5 wt% and with 10 wt% of LDPE/MMT-EU.

Compositions	T _m (°C)	T _c (°C)	ΔH _M (J/g)	ΔH _C (J/g)
LLDPE	125.28	111.85	336.47	-150.11
LLDPE + 5 wt% of LDPE/MMT-EU	124.23	111.88	273.25	-129.00
LLDPE + 10 wt% of LDPE/MMT-EU	125.28	111.88	325.10	-174.78

T_m – Melting Temperature; T_c – Crystallization Temperature; ΔH_M – Melting Enthalpy; ΔH_C – Crystallization Enthalpy

the enthalpy of crystallization increases by 16.40% and the enthalpy of fusion does not change significantly. Studies reported by Silvano et al.⁷ showed that the addition of a low percentage of MMT-EU promotes a decrease in the degree of crystallinity of LLDPE films, similar to the results shown with 5 wt% of LDPE/MMT-EU in this study⁷. The authors reported that erucamide molecules hinder the orientation of LLDPE molecules and increase molecular spacing and reduce the degree of crystallinity of the polymeric matrix. But, when high percentage of MMT-EU nanocomposite is added the crystallization enthalpy increases, indicating an improvement in the compatibility conditions between the erucamide molecules and the LLDPE matrix. The favorable interaction between erucamide molecules and the LLDPE molecules induces an increase in the compatibility between both types of molecules and consequently in the increase of the crystallization degree of the polymeric matrix, according are shown when is added 10 wt% of the LDPE/MMT-EU.

3.2.3. Atomic force microscopy (AFM)

AFM microscopy analyzes were performed 24 hours after film processing. Figure 9 shows the images obtained with samples of LLDPE, LLDPE film with 5 wt% and 10 wt% of LDPE/MMT-EU and the average roughness values for all samples.

The addition of LDPE/MMT-EU promoted the reduction of surface roughness. The decrease in roughness is associated with the compatibility of erucamide molecules (EU) with the LLDPE matrix by the action of montmorillonite (MMT). However, the decrease in roughness is more pronounced with 5 wt% of LDPE/MMT-EU and is in agreement with the results presented by Silvano et al.⁷, who reported a similar effect of the concentration of the MMT-EU on LLDPE films⁷.

The average roughness value for the surface of the LLDPE film is 79.12 nm, while for LLDPE films with 5 wt% of LDPE/MMT-EU and 10 wt% of LDPE/MMT-EU is 68.24 nm and 76.64 nm, respectively. According to Silvano et al.⁷, the reduction in surface roughness is provided by the addition of MMT-EU, which promotes a decrease in the coefficient of friction of LLDPE films^{7,16}.

3.2.4. Contact angle values (CA)

Contact angle (CA) values were determined for the surfaces of LLDPE films and LLDPE films with 5 wt% and 10 wt% of LDPE/MMT-EU. The results show a significant increase in CA values with the addition of MMT-EU. For the surface of LLDPE films with 5% by weight and 10% by weight of LDPE/MMT-EU, the CA values increase by 7.82% and 6.40%, respectively. Figure 10a, 10b and 10c show the images of the contact angle experiments carried out with drops of water.

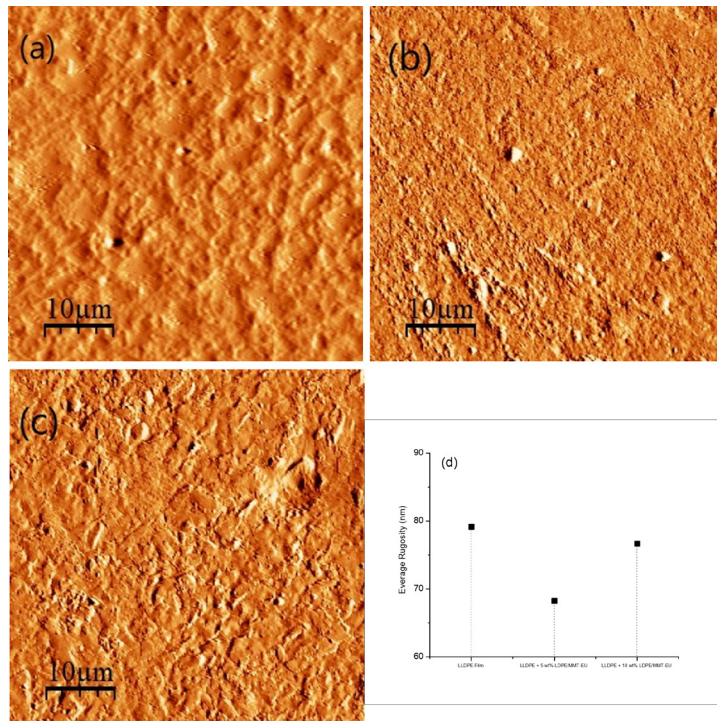


Figure 9. Atomic force images obtained on the (a) LLDPE films, (b) LLDPE films with 5 wt% of LDPE/MMT-EU, (c) LLDPE films with 10 wt% of LDPE/MMT-EU and (d) average roughness value for the surface of the LLDPE with different percentages of LDPE/MMT-EU.

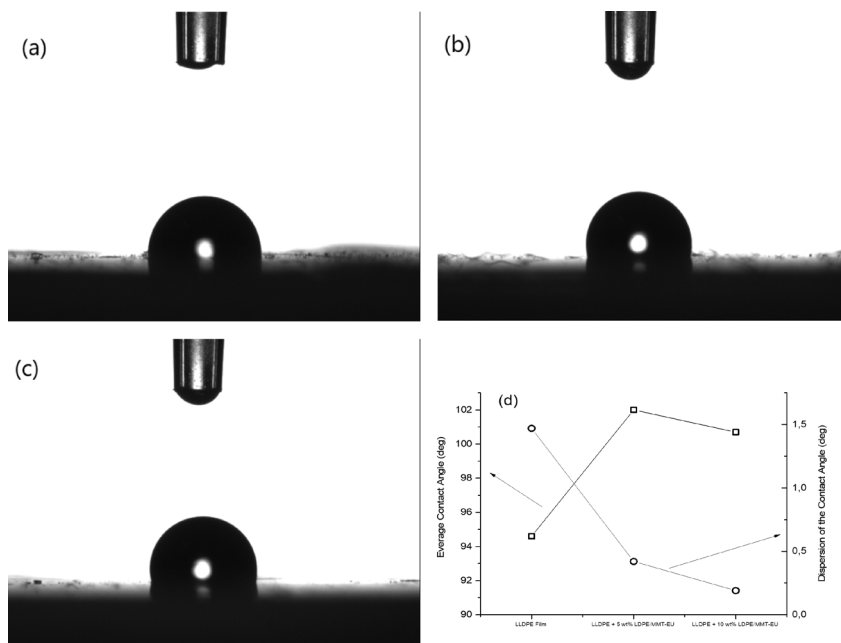


Figure 10. Images from the contact angle experiments with water and LLDPE films. (a) LLDPE Films, (b) LLDPE with 5 wt% of LDPE/MMT-EU, (c) LLDPE with 10 wt% of LDPE/MMT-EU and (d) average contact angle values determined for the water droplets on the LLDPE films surfaces with and without MMT-EU.

Figure 10d shows the increase in contact angle values with the addition of LDPE/MMT-EU and associated with the reduction of dispersion of contact angle values. LLDPE is a nonpolar polymer and naturally manifests its hydrophobic

affinity from contact angle values greater than 94.0°. However, with the addition of MMT-EU, the roughness is reduced (according to AFM images) and the effective area of the contact surface is increased, which provides higher contact

angle values for the LLDPE surfaces with the nanocomposite, 102.0° and 100.7°, respectively. Therefore, the addition of MMT-EU reduces the average roughness and favors the manifestation of the hydrophobic nature of the LLDPE film surfaces. The decrease of the dispersion of the contact angle values is observed with addition of the MMT-EU, that is a strong indicator of the increase of the uniformity of the rugosity on surface. This evidence is according to results reported by Bogdanova et al.¹⁷, that showed that a decrease in the surface roughness corresponds to a decrease in the contact angle dispersion on the polyethylene surfaces¹⁷.

3.2.5. Mechanical tests of the LLDPE films

Force versus displacement diagrams obtained for the LLDPE films and for the LLDPE films with 5 wt% and 10 wt% of LDPE/MMT-EU, all with one welding region, are shown in the Figure 11.

In Figure 12a are shown details of the diagrams for the low displacement values and in Figure 12b are shown the simulated mechanical behavior used to determine the mechanical parameters, by fitting curve achieved from Equation 1. Corresponding statistical tests for the values of the stiffness, strength and ductility are shown in Figure 13. The overall local strains distributions for the LLDPE films close to the welding site, retrieved from the DIC measurements, are displayed in Figure 14.

Mechanical results prove that the addition of MMT-EU nanocomposite improve the overall mechanical behavior of the LLDPE films regarding stiffness, strength and ductility. Moreover, no failures (delamination) were observed in the LLDPE films and in the welding interface after the mechanical tests. Although there is no statistical significance in the stiffness between the LLDPE films with 5 wt% and 10 wt% of LDPE/MMT-EU. It's evident that the stiffness, strength and ductility values increase with the addition of MMT-EU nanocomposite.

Mechanical results showed by the Force versus Displacement Diagrams are according with the strain fields analysis depicted in Figure 14a, where it can be seen that the addition of 10 wt% of the LDPE/MMT-EU significantly

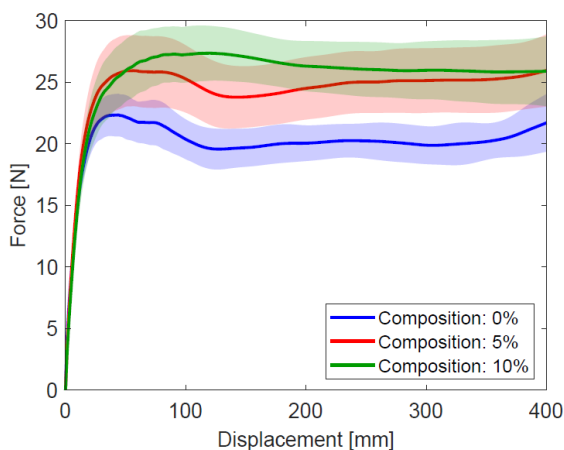


Figure 11. Force versus displacement diagram for LLDPE Films and for LLDPE Films with 5 wt% and 10 wt% of MMT-EU nanocomposite.

reduces the strain concentration in comparison to the LLDPE films and in comparison, with LLDPE with 5 wt% of LDPE/MMT-EU, Figure 14b.

The increase of the stiffness, strength and ductility values of the LLDPE films with the addition of MMT-EU are associated with the improves promoted by the nanocomposites. The montmorillonite in the nanocomposite improve the compatibilization of the erucamide molecules with the LLDPE molecules. It has been proven that the presence of the montmorillonite improves the distribution of the erucamide molecules and reduces the roughness of the polymeric surface due decrease its agglomerate sizes⁷.

It is possible that the lower agglomerates of erucamide molecules and the increase of its compatibility with the LLDPE molecules reduces the number of interfacial defects between erucamide phases and LLDPE phase and the mechanical resistance improves. The presence of the montmorillonite in the MMT-EU nanocomposite increase de mobility of the LLDPE molecules and strength and ductility of the polymeric matrix increase.

An important result is that the mechanical properties of the LLDPE improved with the MMT-EU nanocomposite, but the coefficient of friction not were modified significantly. The function of the erucamide molecules not were modified with the presence of the montmorillonite, in additionally, the mechanical properties of the LLDPE films are improved.

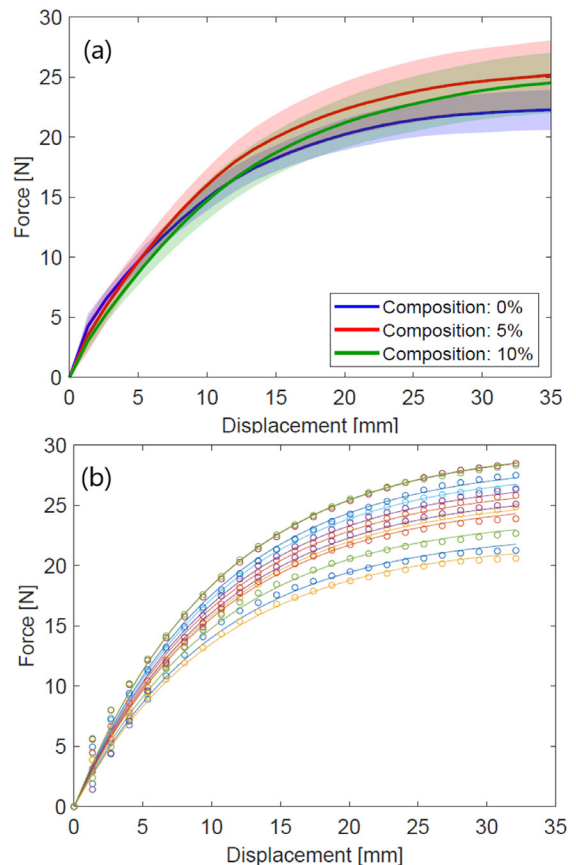


Figure 12. (a) details of the diagrams for low displacements regions and (b) simulated diagrams in low displacement regions used to determine the mechanical parameters.

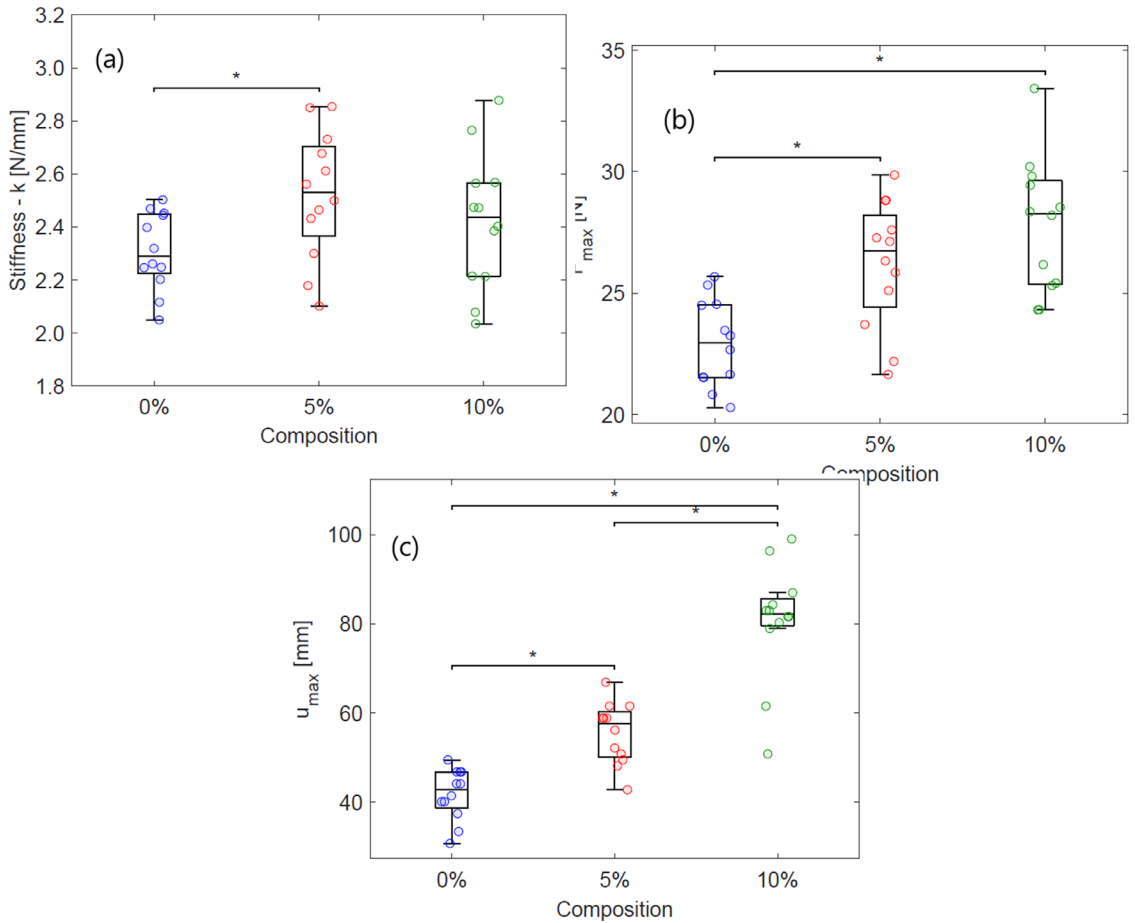


Figure 13. Mechanical properties determined for the LLDPE films and for the LLDPE films with 5 wt% and 10 wt% of MMT-EU nanocomposite, from the analysis of the Force versus Displacement Diagrams. (a) Stiffness values, (b) Maximum Force values and (c) Maximum Deformation values. Significance statistically analyzed for $p < 0.05$.

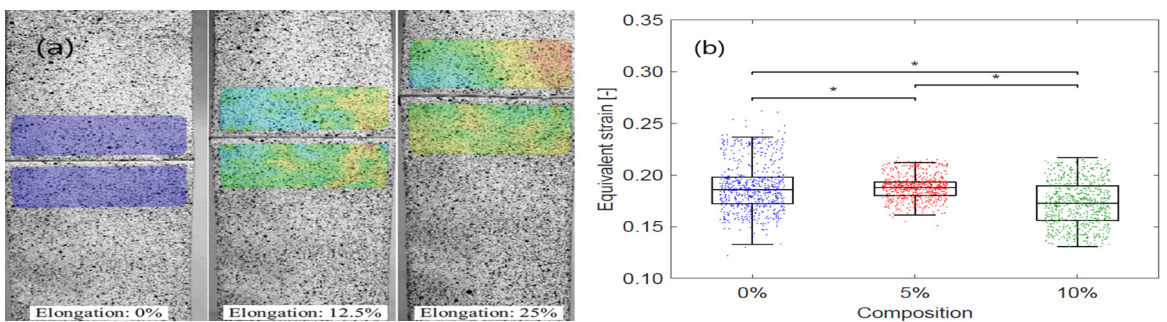


Figure 14. (a) Strain fields within the region of interest (ROI) close of the welding regions and (b) equivalent strain for the LLDPE films and for the LLDPE films with 5 wt% and 10 wt% of MMT-EU nanocomposite. Statistical significance: $p < 0.05$.

4. Conclusion

The incorporation of the MMT-EU nanocomposite improved the mechanical properties of the LLDPE films, with emphasis on the stiffness, strength and ductility values. The results show a significant increase in contact angle values with increasing MMT-EU concentration, in addition to reducing

the mean roughness of LLDPE films and the dispersion of contact angle values. These results are strong indicators that the MMT-EU favors the uniformity of roughness on the surface of LLDPE films and hydrophobicity.

Thus, the MMT-EU nanocomposite can be considered an important additive to improve the mechanical properties and the decrease the roughness of the LLDPE films.

5. Acknowledgments

The authors would like to thank the following agencies and personnel: Community University of Chapecó Region; CNPq and CAPES for the financing support, UNIEDU-SC program. The authors are thankful for the Multi-User Facility infrastructure from Santa Catarina State University's Technological Sciences Center.

6. References

1. Gubala D, Harniman R, Eloi J-C, Wąsik P, Wermeille D, Sun L et al. Multiscale characterisation of single synthetic fibres: surface morphology and nanomechanical properties. *J Colloid Interface Sci.* 2020;571:398-411.
2. Dulal N, Shanks R, Gengenbach T, Gill H, Chalmers D, Adhikari B et al. Slip-additive migration, surface morphology, and performance on injection moulded high-density polyethylene closures. *J Colloid Interface Sci.* 2017;505:537-45.
3. Molnar NM. Erucamide. *J Am Oil Chem Soc.* 1974;51(3):84-7.
4. Ramirez MX, Hirt DE, Wright LL. AFM characterization of surface segregated erucamide and behenamide in linear low-density polyethylene film. *Nano Lett.* 2002;2(1):9-12.
5. Llop C, Manrique A, Navarro R, Mijangos C, Reinecke H. Control of the migration behavior of slip agents in polyolefin-based films. *Polym Eng Sci.* 2011;51(9):1763-9.
6. Ramirez MX, Walters KB, Hirt DE. Relationship between erucamide surface concentration and coefficient of friction of LLDPE film. *J Vinyl Addit Technol.* 2005;11(1):9-12.
7. Silvano JR, Santa RAAB, Martins MAPM, Riella HG, Soares C, Fiori MA. Nanocomposite of erucamide-clay applied for the control of friction coefficient in surfaces of LLDPE. *Polym Test.* 2018;67:1-6.
8. Llop C, Manrique A, Navarro R, Mijangos C, Reinecke H. Control of the migration behavior of slip agents in polyolefin-based films. *Polym Eng Sci.* 2011;51(9):1763-9.
9. Tiwari RR, Natajara U. Effect of organic modification on the intercalation and the properties of poly(phenylene oxide)/polystyrene blend-clay nanocomposites. *J Thermoplast Compos Mater.* 2012;26(3):392-415.
10. Gautam A, Komal P. Synthesis of montmorillonite clay/poly(vinyl alcohol) nanocomposites and their mechanical properties. *J Nanosci Nanotechnol.* 2019;19(12):8071-7.
11. Silvano JR, Mello JMM, Silva LL, Riella HG, Fiori MA. Erucamide-nanoclay systems obtained by intercalation process. *Mater Sci Forum.* 2017;899:36-41.
12. Holzapfel GA. *Nonlinear solid mechanics.* Chichester: Wiley; 2000.
13. Zagho MM, Khader MM. The impact of clay loading on the relative intercalation of poly(vinyl alcohol)-clay composites. *J Mater Sci Chem Engin.* 2016;4:20-31.
14. Velasco-Ruiz MF, Quijada-Garridor I, Benavente R, Barrales-Rienda JM. Miscibility studies of erucamide (13-cis-docosenamide)/poly(lauro lactam) (nylon 12) (PA-12) blends. *Polymer.* 2000;41:5819-28.
15. Sankhe SY, Janorkar AV, Hirt DE. Characterization of erucamide profiles in LLDPE films: depth-profiling attempts using FTIR photoacoustic spectroscopy and Raman microspectroscopy. *J Plast Film Sheeting.* 2003;19(1):16-29.
16. Lin Y, Bilotti E, Bastiaansen CWM, Peijs T. Transparent semi-crystalline polymeric materials and their nanocomposites: a review. *Polym Eng Sci.* 2020;60:2351-76.
17. Bogdanova YG, Dolzhikova VD, Tsvetkova DS, Karzov IM, Alent'ev AY. Contact angles as indicators of the polymer surface structure. *J Struct Chem.* 2011;52(6):1187-94.